Reversible Near-Infrared/Blue Mechanofluorochromism of Aminobenzopyranoxanthene

ARTICLE *in* JOURNAL OF THE AMERICAN CHEMICAL SOCIETY · MAY 2015

Impact Factor: 12.11 · DOI: 10.1021/jacs.5b00877 · Source: PubMed

JACS
JOURNAL OF THE AMERICAN CHEMICAL SOCIETY

Communication

pubs.acs.org/JACS

Reversible Near-Infrared/Blue Mechanofluorochromism of Aminobenzopyranoxanthene

Masaru Tanioka,[†,‡] Shinichiro Kamino,*[,†,‡] Atsuya Muranaka,*[,§] Yousuke Ooyama,[∥] Hiromi Ota,[⊥] Yoshinao Shirasaki,[▽] Jun Horigome,[#] Masashi Ueda,[†] Masanobu Uchiyama,[§,▽] Daisuke Sawada,[†] and Shuichi Enomoto*[,†,‡]

[†]Graduate School of Medicine, Dentistry, and Pharmaceutical Sciences and [⊥]Division of Instrumental Analysis, Department of Instrumental Analysis and Cryogenics, Advanced Science Research Center, Okayama University, Okayama-shi, Okayama 700-8530, Japan

[‡]Next-generation Imaging Team, RIKEN-CLST, Kobe-shi, Hyogo 650-0047, Japan

[§]Advanced Elements Chemistry Research Team and Elements Chemistry Laboratory, RIKEN-CSRS, Wako-shi, Saitama 351-0198, Japan

[∥]Department of Applied Chemistry, Graduate School of Engineering, Hiroshima University, Higashi-Hiroshima, Hiroshima 739-8527, Japan

[▽]Graduate School of Pharmaceutical Sciences, The University of Tokyo, 7-3-1 Hongo, Bunkyo-ku, Tokyo 113-0033, Japan

[#]Hitachi High-Tech Science Co., Ltd., Hitachinaka-shi, Ibaraki 312-8504, Japan

Supporting Information

ABSTRACT: Mechanochromic organic molecules (MOMs) that exhibit a large difference of fluorescence wavelength between two states have important potential applications, but few such compounds are known. Here, we report a new MOM, *cis*-ABPX01^0, which shows switchable near-IR and blue fluorescence responses. Detailed spectrophotometric and single-crystal X-ray analyses revealed that the near-IR fluorescence is attributable to fluorescence from slip-stacked dimeric structures in crystals, while the blue fluorescence is attributable to fluorescence from the monomer. Switching between the two is achieved by dynamic structural interconversion between the two molecular packing arrangements in response to mechanical grinding and solvent vapor-fuming.

Mechanochromic organic molecules (MOMs), which change their intrinsic optical properties in response to external stimuli such as mechanical grinding and pressure, have sparked tremendous interest because of their potential for various applications involving sensors, memory devices, and optical displays.[1] A promising strategy to tune the optical properties of MOMs is control of molecular packing, because solid-state optical properties strongly depend on molecular packing arrangements. Therefore, various types of MOMs that can change their molecular packing structures have been designed and synthesized to date.[2] Most of these molecules exhibit absorption and/or fluorescence bands in the UV−vis region. Although near-IR technologies are of greatest interest for their potential applications such as information security, medical imaging, and photodynamic treatment,[3] near-IR responsive materials are rare.[4] Further, MOMs with a large difference between the fluorescence peaks in the two states are especially required for practical applications.[5]

Aminobenzopyranoxanthenes (ABPXs), recently developed by our group,[6] exhibit unique fluorescence and coloration characteristics in solution as a result of multistep structural changes of three equilibrium species through a spiro-ring opening/closing process in response to chemical stimuli (see Scheme S1 in the Supporting Information (SI)).[7] While continuing to explore their unique physical/chemical properties, we serendipitously discovered that one spirolactone form of ABPXs, *cis*-ABPX01^0, is a new type of MOM with a large wavelength difference of fluorescence (near-IR/blue) between two states in the crystal (Figure 1a). Herein, we report on the unique optical properties of *cis*-ABPX01^0 and the relationship between the molecular packing arrangement and the dual fluorescence character.

cis- and *trans*-ABPX01^0 were synthesized by condensation of 2-[4-(diethylamino)-2-hydroxybenzoyl]benzoic acid with resorcinol in CH_3SO_3H under heating.[6,7] Single crystals of *cis*-ABPX01^0 were prepared by slow diffusion of less solubilizing solvent EtOAc into a solution of the compound in more solubilizing solvent CH_2Cl_2. X-ray crystallography showed that the crystal included CH_2Cl_2 molecules in the lattice. The obtained clathrate crystals of *cis*-ABPX01^0/CH_2Cl_2 ($\mathbf{1}_{cis}$) were colorless under ambient light and appeared deep purple under UV irradiation (Figure 1b). The solid-state fluorescence and absorption spectra of $\mathbf{1}_{cis}$ are shown in Figure 1c. The absorption of $\mathbf{1}_{cis}$ appeared in the ultraviolet (<400 nm) region, and $\mathbf{1}_{cis}$ showed blue fluorescence at around 450 nm upon excitation at 365 nm. More importantly, $\mathbf{1}_{cis}$ exhibited near-IR fluorescence (λ_{max} = 758 nm) with a very large Stokes shift of ~400 nm (15000 cm^{-1}) from the UV absorption. The quantum

Received: January 28, 2015
Published: May 12, 2015

DOI: 10.1021/jacs.5b00877
J. Am. Chem. Soc. 2015, 137, 6436−6439

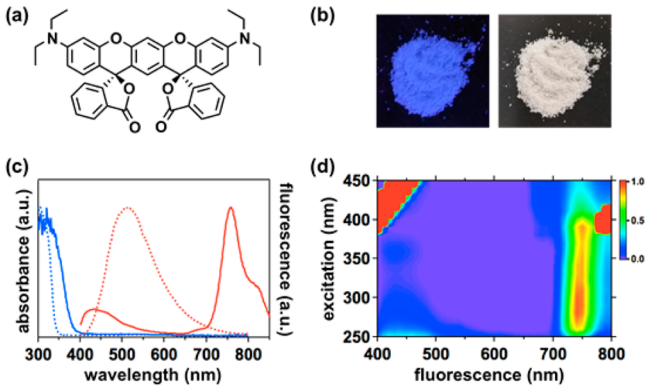

Figure 1. (a) Chemical structure of *cis*-ABPX01^0. (b) Photographs of $\mathbf{1}_{cis}$ obtained by slow diffusion of EtOAc into a CH_2Cl_2 solution under 365 nm irradiation (left panel) and under ambient light (right panel). (c) Fluorescence (red line) and absorption (blue line) spectra of *cis*-ABPX01^0 in CH_2Cl_2 solution (dotted line) and $\mathbf{1}_{cis}$ (solid line). (d) Fluorescence−excitation matrix spectrum of $\mathbf{1}_{cis}$.

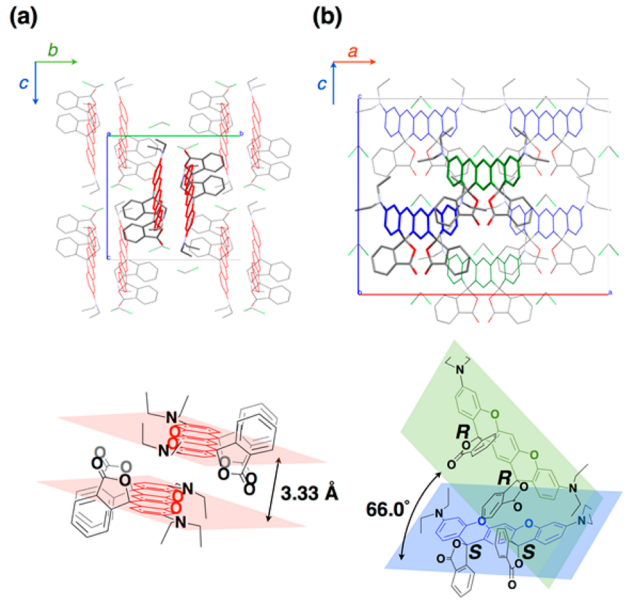

Figure 2. Crystal packing structures of (a) *cis*-ABPX01^0/CH_2Cl_2 $\mathbf{1}_{cis}$ and (b) *trans*-ABPX01^0/CH_2Cl_2 $\mathbf{1}_{trans}$ co-crystallized with CH_2Cl_2. The xanthene ring of $\mathbf{1}_{cis}$ is shown in red and forms a slipped, stacking dimer unit with close contacts (in the range of 3.33 Å). The xanthene ring of $\mathbf{1}_{trans}$ exists independently as a monomer unit due to separation of *R,R* (green) and *S,S* (blue). Hydrogen atoms are omitted for clarity.

yield of the whole fluorescence region was 0.009. Fluorescence−excitation matrix (FEM) spectrophotometry of $\mathbf{1}_{cis}$ was conducted to examine the relationship between the fluorescence and absorption bands. The FEM spectrum clearly indicates that near-IR fluorescence is observed upon excitation in the whole region of the absorption band of *cis*-ABPX01^0 (Figure 1d). The near-IR fluorescence was not observed in CH_2Cl_2 solution, while 100 μM *cis*-ABPX01^0 showed a broad absorption band with the maximum at 305 nm, only blue-green fluorescence was observed with the maximum wavelength of 514 nm (Figure 1c). Even at high concentration (<50 mM), no near-IR fluorescence was observed (Figure S1). This raises the question, what causes the near-IR fluorescence of the *cis*-ABPX01^0 crystal.

Figure 2a shows the molecular packing structure of $\mathbf{1}_{cis}$ (see the SI for crystallographic data of all crystals). *cis*-ABPX01^0 in $\mathbf{1}_{cis}$ forms intermolecular C−H···O hydrogen bonds (2.31 and 2.57 Å) and C−Cl···π interactions (3.32 Å) with CH_2Cl_2 molecule. *cis*-ABPX01^0 in the $\mathbf{1}_{cis}$ crystal adopted a distinct slip-stacked dimer structure with a considerable offset. The intermolecular distance between the xanthene rings (C1−C41), as determined by the least-squares method, was 3.33 Å, which is shorter than the sum of the van der Waals radii of the C atoms (3.4 Å). These antiparallel dimeric units were linearly arranged without evident intermolecular interactions.

The remarkable near-IR fluorescence is unique to $\mathbf{1}_{cis}$. The absorption spectrum of the crystal of *trans*-ABPX01^0/CH_2Cl_2 ($\mathbf{1}_{trans}$) is similar to that of $\mathbf{1}_{cis}$, but $\mathbf{1}_{trans}$ exhibited only blue fluorescence (Figure S3). C−Cl···π interactions (3.25 Å) were observed for *trans*-ABPX01^0 in $\mathbf{1}_{trans}$ with CH_2Cl_2 molecule. As shown in Figure 2b, the crystal is composed of the racemic forms of the enantiomers. The dihedral angles of the two xanthene rings of the *R,R* and *S,S* forms were 66.0°, so that *trans*-ABPX01^0 in $\mathbf{1}_{trans}$ did not adopt a slip-stacked dimeric structure like that of $\mathbf{1}_{cis}$. These results indicated that the near-IR fluorescence might be derived from the dimer configuration with close packing of the two xanthene rings, while the blue fluorescence is derived from the monomer configuration of ABPX01^0.

To gain direct evidence in support of this hypothesis, we prepared clathrate crystals having different molecular packing arrangements of *cis*-ABPX01^0 by the inclusion of various solvents, and we carefully investigated their fluorescence behaviors and structural characteristics. Figure 3 summarizes the relationship between molecular packing structure and solid-state spectra for *cis*-ABPX01^0. The absorption bands of all crystals mainly appeared in the ultraviolet region.

Crystals of *cis*-ABPX01^0/$CHCl_3$ ($\mathbf{2}_{cis}$), *cis*-ABPX01^0/THF ($\mathbf{3}_{cis}$), *cis*-ABPX01^0/EtOH ($\mathbf{4}_{cis}$), and *cis*-ABPX01^0/1,2-DCE ($\mathbf{5}_{cis}$) exhibited dual near-IR and blue fluorescence. Most of solvent molecules in the four crystals were localized near the spirolactone moiety of *cis*-ABPX01^0. The xanthene ring was spatially open to form the close slip-stacked dimers with a considerable offset. The interplanar distances were 3.29−4.86 Å, and the dimeric unit was independently formed. The xanthene ring of $\mathbf{3}_{cis}$ had high torsional strain, whereas the xanthene moiety of the other crystals showed a high degree of planarity. It is noteworthy that the peak position of the near-IR fluorescence remained unchanged despite the inclusion of different solvent molecules. On the other hand, the clathrate crystals of *cis*-ABPX01^0/cyclohexane ($\mathbf{6}_{cis}$) and *cis*-ABPX01^0/Et_2O ($\mathbf{7}_{cis}$), *cis*-ABPX01^0/CCl_4 ($\mathbf{8}_{cis}$) showed blue fluorescence in the monomeric configuration. The X-ray crystallographic analyses support the idea that the crystal structure composed of dimers with close stacking of the xanthene rings (interfacial distance of <5 Å) is important for near-IR fluorescence.

To explain these results, we first considered that the near-IR luminescent band is due to the formation of two triplet excitons, because slip-stacked dimer structure facilitates a singlet fission process.[8] The spirolactone form of rhodamine 101 is known to exhibit phosphorescence at ~670 nm in frozen solution.[9] However, the fluorescence lifetime values (τ_{obs} = 2.71, 8.23 ns) for $\mathbf{1}_{cis}$ at 740 nm indicated that the near-IR luminescence is attributed to the singlet excited state fluorescence (see Table S3 of the photophysical properties of all crystals). Excimer formation between spirolactone forms was considered as a possible origin, as is the case in pyrene-based

DOI: 10.1021/jacs.5b00877
J. Am. Chem. Soc. 2015, 137, 6436−6439

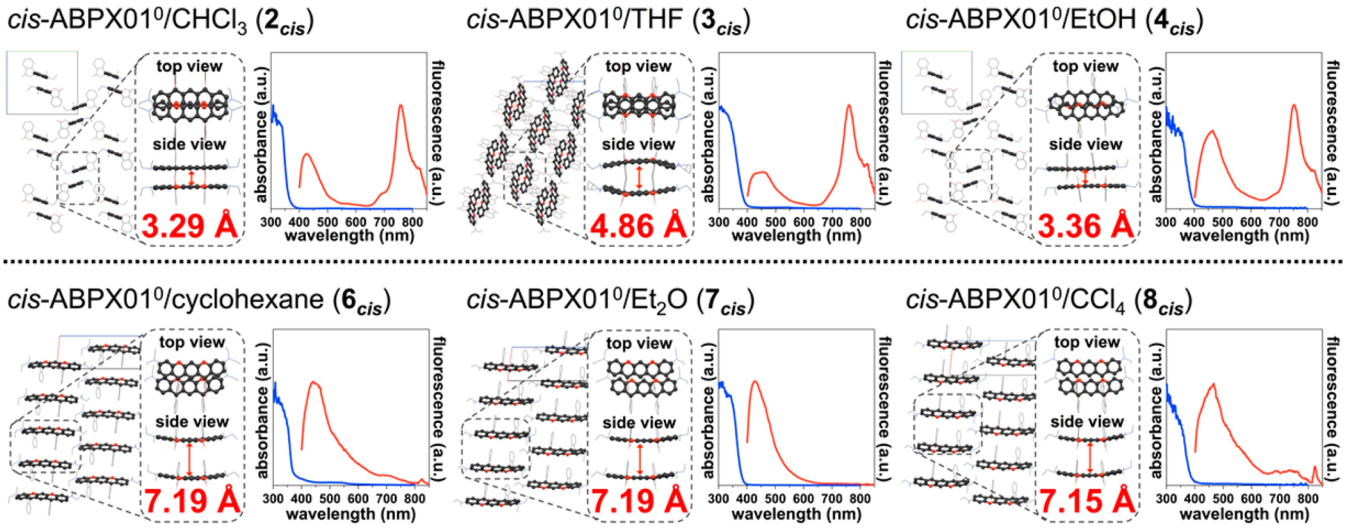

Figure 3. Relationship between solvent-inclusion-dependent molecular packing structure and solid-state spectra of $\mathbf{2}_{cis}$, $\mathbf{3}_{cis}$, $\mathbf{4}_{cis}$, $\mathbf{6}_{cis}$, $\mathbf{7}_{cis}$, and $\mathbf{8}_{cis}$ (see Figure S11 for the data of *cis*-ABPX01^0/1,2-DCE $\mathbf{5}_{cis}$). Solvent molecules and hydrogen atoms are omitted for clarity. Left panels show the crystal structures of $\mathbf{2}_{cis}$–$\mathbf{8}_{cis}$. Right panels show fluorescence (red line) and absorption (blue line) spectra of these crystals. $\mathbf{2}_{cis}$, $\mathbf{3}_{cis}$, and $\mathbf{4}_{cis}$ exhibit dual near-IR and blue fluorescence, while $\mathbf{6}_{cis}$, $\mathbf{7}_{cis}$ and $\mathbf{8}_{cis}$ show blue fluorescence.

MOMs,[2e,10] but the large spectral shift and relatively sharp band are not typically seen in the case of excimer fluorescence.

We consider that the near-IR fluorescence is related to the structural changes through the temporary spiro-ring opening/closing process by photoexcitation (see Figure S18). It was found that spiro C–O bond lengths of near-IR-emissive crystals were somewhat longer than those of blue-emissive ones (Table S4). The longer C–O bond length may give easy cleavage of the bond upon excitation to open the spiro-ring resulting in quinoidal zwitterionic form. When $\mathbf{1}_{cis}$ was irradiated upon the xenon lamp light at 365 nm, the temporary coloration of $\mathbf{1}_{cis}$ at the irradiated spot was indeed observed, and the intensity of near-IR fluorescence at 750 nm was saturated within 10 s. These preliminary results suggest that more or less colored zwitterionic forms of ABPX01$^{\pm}$ or ABPX01$^{2\pm}$ are photochemically generated, as is seen in conventional rhodamines,[11] from the colorless ABPX01^0 dimer. We calculated the absorption spectra of the monomeric and dimeric configurations extracted from the crystallographic data of $\mathbf{2}_{cis}$ (in which the intermolecular distance between two xanthene rings is the shortest) and $\mathbf{6}_{cis}$ (in which the distance is the longest).[12] No visible or near-IR absorption was predicted for any configurations of the spirolactone form, which supports the above interpretation (see Figure S19).

Surprisingly, we found that the dual blue and near-IR fluorescence of $\mathbf{1}_{cis}$ is changed by external stimuli, i.e., mechanical grinding and subsequent solvent vapor fuming, as shown in Figure 4a. When $\mathbf{1}_{cis}$ was ground in a mortar, the near-IR fluorescence was suppressed and the blue fluorescence was enhanced with increasing the grinding time. The absorption band remained in the ultraviolet region after grinding of $\mathbf{1}_{cis}$ (see Figure S21), and the fluorescence color was altered from deep purple to sky blue (Figure 4b and video in the SI). The powder X-ray diffraction (XRD) pattern of ground $\mathbf{1}_{cis}$ did not show noticeable reflection peaks compared with the XRD pattern of $\mathbf{1}_{cis}$ (Figure 4c). It is noted that the grinding-dependent fluorescence and morphological changes were similarly observed in the solvent-desorbed crystals of $\mathbf{1}_{cis}$, which are indicative of mechanofluorochromism of $\mathbf{1}_{cis}$ (see Figures S22–S23). The crystalline form was restored by fuming

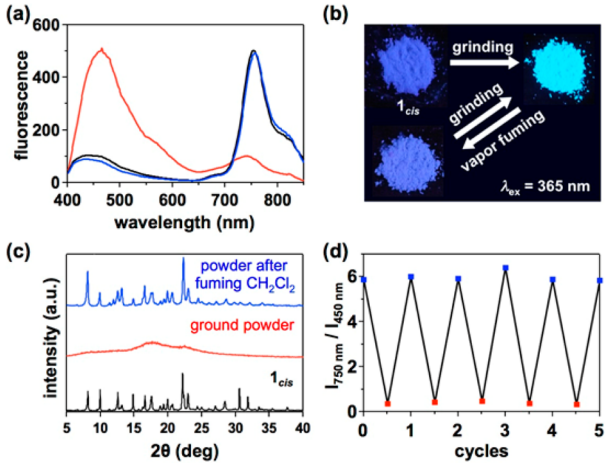

Figure 4. (a) Solid-state fluorescence spectra of $\mathbf{1}_{cis}$. The fluorescence intensities at 450 and 750 nm were not normalized. Black: $\mathbf{1}_{cis}$. Red: ground powder of $\mathbf{1}_{cis}$. Blue: powder after fuming CH_2Cl_2 for 3 h. (b) Photographs were taken in a mortar under 365 nm irradiation. (c) Powder XRD patterns of $\mathbf{1}_{cis}$. (d) Fluorescence repeatability of the response of $\mathbf{1}_{cis}$ to external stimuli of grinding and CH_2Cl_2 fuming.

the ground powder of $\mathbf{1}_{cis}$ with CH_2Cl_2. ^{1}H NMR spectra of $\mathbf{1}_{cis}$ in $CDCl_3$ indicate that mechanical grinding induces desorption of CH_2Cl_2 molecules from $\mathbf{1}_{cis}$. CH_2Cl_2 molecules were subsequently resorbed by ground powder of $\mathbf{1}_{cis}$ upon CH_2Cl_2 fuming (see Figure S24). These results also suggest that the near-IR fluorescence changes are related to the crystalline dimer structure. Other clathrate crystals of $\mathbf{2}_{cis}$–$\mathbf{8}_{cis}$ exhibited the mechanofluorochromic properties, although their near-IR fluorescence intensity was weaker than $\mathbf{1}_{cis}$. (see Figure S25). We next investigated the "fluorescence repeatability" of the mechanochromic response of $\mathbf{1}_{cis}$. The ratio of fluorescence intensity at 750 nm to that at 450 nm was reproducible over at least five cycles under our conditions[13] (Figure 4d). A ratiometric detection system utilizing this dual fluorescence would be useful for precise sensing to eliminate background noise arising from the matrix. Furthermore, the near-IR-emissive crystals of $\mathbf{1}_{cis}$–$\mathbf{5}_{cis}$ were stable when the crystals were

DOI: 10.1021/jacs.5b00877
J. Am. Chem. Soc. 2015, 137, 6436–6439

exposed to high temperature conditions (see Figure S26). *cis*-ABPX01^0 is a mechano- and vapofluorochromic material that is characterized by the reversible structural conversion between dimer and monomer by grinding and fuming with solvent molecule.[12]

In conclusion, *cis*-ABPX01^0 is a new type of MOM with a remarkable dual fluorescence characteristic. Several clathrate crystals of *cis*-ABPX01^0 exhibit a sharp near-IR fluorescence band despite the fact that no absorption band is seen in the visible-near-IR region. X-ray analysis of clathrate crystals with various solvents revealed that slip-stacked dimer structure is related to the near-IR fluorescence. The fluorescence properties can be reproducibly cycled by repeated mechanical grinding and solvent vapor fuming. We are currently investigating several applications of ABPXs as well as the origin of the near-IR fluorescence of *cis*-ABPX01^0 dimer.

■ ASSOCIATED CONTENT

Supporting Information

Experimental detail and additional data. The Supporting Information is available free of charge on the ACS Publications website at DOI: 10.1021/jacs.5b00877.

■ AUTHOR INFORMATION

Corresponding Authors

*skamino@cc.okayama-u.ac.jp
*atsuya-muranaka@riken.jp
*senomoto@pharm.okayama-u.ac.jp

Notes

The authors declare no competing financial interest.

■ ACKNOWLEDGMENTS

This work was supported by the Adaptable and Seamless Technology Transfer Program through Target-driven R&D (Grant AS262Z02786M) of Japan Science and Technology (JST). This research was also supported in part by RIKEN Junior Research Associate Program. We would also like to thank Dr. Toshihiro Shirasaki of Hitachi High-Tech Science Co., Ltd. for support with fluorescent analysis, Dr. Kengo Suzuki of Hamamatsu Photonics Co., Ltd. for support with fluorescent lifetime and quantum yields measurement, and Mr. Toshiaki Enoki of Hiroshima University for support with TG-DTA measurement.

■ REFERENCES

(1) (a) Chan, E. P.; Walish, J. J.; Thomas, E. L.; Stafford, C. M. *Adv. Mater.* **2011**, *23*, 4−702−4706. (b) Ciardelli, F.; Ruggeri, G.; Pucci, A. *Chem. Soc. Rev.* **2013**, *42*, 857−870. (c) Cellini, F.; Khapli, S.; Peterson, S. D.; Porfiri, M. *Appl. Phys. Lett.* **2014**, *105*, 061907. (d) Park, D. H.; Hong, J.; Park, I. S.; Lee, C. W.; Kim, J. M. *Adv. Funct. Mater.* **2014**, *24*, 5186−5193. (e) Sun, H. B.; Liu, S. J.; Lin, W. P.; Zhang, K. Y.; Lv, W.; Huang, X.; Huo, F. W.; Yang, H. R.; Jenkins, G.; Zhao, Q.; Huang, W. *Nat. Commun.* **2014**, *5*, 3601−3609. (f) Wang, X. Q.; Wang, C. F.; Zhou, Z. F.; Chen, S. *Adv. Opt. Mater.* **2014**, *2*, 652−662. (g) Wu, Y.; Hu, J. L.; Huang, H. H.; Li, J.; Zhu, Y.; Tang, B. Z.; Han, J. P.; Li, L. B. *J. Polym. Sci., Part B: Polym. Phys.* **2014**, *52*, 104−110. (h) Yang, D. P.; Ye, S. Y.; Ge, J. P. *Adv. Funct. Mater.* **2014**, *24*, 3197−3205.

(2) (a) Zhang, G. Q.; Lu, J. W.; Sabat, M.; Fraser, C. L. *J. Am. Chem. Soc.* **2010**, *132*, 2160−2162. (b) Ooyama, Y.; Harima, Y. *J. Mater. Chem.* **2011**, *21*, 8372−8380. (c) Sagara, Y.; Kato, T. *Angew. Chem., Int. Ed.* **2011**, *50*, 9128−9132. (d) Wang, J.; Mei, J.; Hu, R. R.; Sun, J. Z.; Qin, A. J.; Tang, B. Z. *J. Am. Chem. Soc.* **2012**, *134*, 9956−9966. (e) Chi, Z. G.; Zhang, X. Q.; Xu, B. J.; Zhou, X.; Ma, C. P.; Zhang, Y.; Liu, S. W.; Xu, J. R. *Chem. Soc. Rev.* **2012**, *41*, 3878−3896. (f) Nagura, K.; Saito, S.; Yusa, H.; Yamawaki, H.; Fujihisa, H.; Sato, H.; Shimoikeda, Y.; Yamaguchi, S. *J. Am. Chem. Soc.* **2013**, *135*, 10322−10325. (g) Metz, A. E.; Podlesny, E. E.; Carroll, P. J.; Klinghoffer, A. N.; Kozlowski, M. C. *J. Am. Chem. Soc.* **2014**, *136*, 10601−10604. (h) Galer, P.; Korosec, R. C.; Vidmar, M.; Sket, B. *J. Am. Chem. Soc.* **2014**, *136*, 7383−7394. (i) Li, G. C.; Song, F. J.; Wu, D.; Lan, J. B.; Liu, X. Y.; Wu, J.; Yang, S. J.; Xiao, D.; You, J. S. *Adv. Funct. Mater.* **2014**, *24*, 747−753. (j) Misra, R.; Jadhav, T.; Dhokale, B.; Mobin, S. M. *Chem. Commun.* **2014**, *50*, 9076−9078. (k) Yagai, S.; Okamura, S.; Nakano, Y.; Yamauchi, M.; Kishikawa, K.; Karatsu, T.; Kitamura, A.; Ueno, A.; Kuzuhara, D.; Yamada, H.; Seki, T.; Ito, H. *Nat. Commun.* **2014**, *5*, 4013−4022. (l) Fan, G. L.; Yan, D. P. *Sci. Rep.* **2014**, *4*, 4933−4940.

(3) (a) Knoll, P. M. *Soc. Inf. Disp. Int. Symp. Dig. Tech. Pap.* **2006**, *37*, 1991−1994. (b) Qian, G.; Wang, Z. Y. *Chem. -Asian J.* **2010**, *5*, 1006−1029. (c) Bünzli, J.-C. G.; Eliseeva, S. V. *Chem. Sci.* **2013**, *4*, 1939−1949. (d) Cheng, L.; Wang, C.; Feng, L. Z.; Yang, K.; Liu, Z. *Chem. Rev.* **2014**, *114*, 10869−10939.

(4) (a) Cheng, X.; Li, D.; Zhang, H.; Wang, Y. *Org. Lett.* **2014**, *16*, 880−883. (b) Xiao, Q.; Zheng, J.; Li, M.; Zhan, S. Z.; Wang, J. H.; Li, D. *Inorg. Chem.* **2014**, *53*, 11604−11615.

(5) (a) Yuan, W. Z.; Tan, Y. Q.; Gong, Y. Y.; Lu, P.; Lam, J. W. Y.; Shen, X. Y.; Feng, C. F.; Sung, H. H. Y.; Lu, Y. W.; Williams, I. D.; Sun, J. Z.; Zhang, Y. M.; Tang, B. Z. *Adv. Mater.* **2013**, *25*, 2837−2843. (b) Sun, J. W.; Lv, X. J.; Wang, P. J.; Zhang, Y. J.; Dal, Y. Y.; Wu, Q. C.; Mi, O. Y.; Zhang, C. *J. Mater. Chem. C* **2014**, *2*, 5365−5371. (c) Xue, P. C.; Chen, P.; Jia, J. H.; Xu, Q. X.; Sun, J. B.; Yao, B. Q.; Zhang, Z. Q.; Lu, R. *Chem. Commun.* **2014**, *50*, 2569−2571.

(6) Kamino, S.; Horio, Y.; Komeda, S.; Minoura, K.; Ichikawa, H.; Horigome, J.; Tatsumi, A.; Kaji, S.; Yamaguchi, T.; Usami, Y.; Hirota, S.; Enomoto, S.; Fujita, Y. *Chem. Commun.* **2010**, *46*, 9013−9015.

(7) (a) Kamino, S.; Muranaka, A.; Murakami, M.; Tatsumi, A.; Nagaoka, N.; Shirasaki, Y.; Watanabe, K.; Yoshida, K.; Horigome, J.; Komeda, S.; Uchiyama, M.; Enomoto, S. *Phys. Chem. Chem. Phys.* **2013**, *15*, 2131−2140. (b) Shirasaki, Y.; Kamino, S.; Tanioka, M.; Watanabe, K.; Takeuchi, Y.; Komeda, S.; Enomoto, S. *Chem.−Asian J.* **2013**, *8*, 2609−2613. (c) Kamino, S.; Murakami, M.; Tanioka, M.; Shirasaki, Y.; Watanabe, K.; Horigome, J.; Ooyama, Y.; Enomoto, S. *Org. Lett.* **2014**, *16*, 258−261.

(8) Smith, M. B.; Michl, J. *Chem. Rev.* **2010**, *110*, 6891−6936.

(9) Karpiuk, J.; Grabowski, Z. R.; Schryver, F. C. *J. Phys. Chem.* **1994**, *98*, 3247−3256.

(10) (a) Yamaguchi, S.; Yoshikawa, I.; Mutai, T.; Araki, K. *J. Mater. Chem.* **2012**, *22*, 20065−20070. (b) Yuan, M. S.; Wang, D. E.; Xue, P. C.; Wang, W. J.; Wang, J. C.; Tu, Q.; Liu, Z. Q.; Liu, Y.; Zhang, Y. R.; Wang, J. Y. *Chem. Mater.* **2014**, *26*, 2467−2477.

(11) (a) Knauer, K. H.; Gleiter, R. *Angew. Chem., Int. Ed.* **1977**, *16*, 113−113. (b) Li, K.; Xiang, Y.; Wang, X.; Li, J.; Hu, R.; Tong, A.; Tang, B. Z. *J. Am. Chem. Soc.* **2014**, *136*, 1643−1649. (c) Uno, S.; Kamiya, M.; Yoshihara, T.; Sugawara, K.; Okabe, K.; Tharhan, M. C.; Fujita, H.; Funatsu, T.; Okada, Y.; Tobita, S.; Urano, Y. *Nat. Chem.* **2014**, *6*, 681−689.

(12) (a) Ni, J.; Wu, Y. H.; Zhang, X.; Li, B.; Zhang, L. Y.; Chen, Z. N. *Inorg. Chem.* **2009**, *48*, 10202−10210. (b) Ni, J.; Zhang, X.; Wu, Y. H.; Zhang, L. H.; Chen, Z. N. *Chem. -Eur. J.* **2011**, *17*, 1171−1183.

(13) Crystal powder of $\mathbf{1}_{cis}$ (100 mg) was ground to an amorphous state over 30 min in an agate mortar. The fluorescence spectrum of the ground powder of $\mathbf{1}_{cis}$ was measured. The agate mortar was placed in a 1 L glass beaker containing 10 mL CH_2Cl_2. The beaker was sealed and left to stand in the dark for 3 h. The mortar was then removed, and the fluorescence spectrum of the vapor-fumed powder was immediately measured. This experimental cycle was repeated five times.

DOI: 10.1021/jacs.5b00877
J. Am. Chem. Soc. 2015, 137, 6436−6439